Supporting Material

Co-translational protein folding within the ribosome tunnel influences trigger-factor recruitment

Ku-Feng Lin[†], Chia-Sui Sun[†,‡], Yi-Chen Huang[†,¶], Sunney I. Chan[†], Jiri Koubek[§,□], Tzong-Huah Wu[†], and Joseph J.-T. Huang[†,*]

[†]Institute of Chemistry, [‡]Molecular Medicine Program, Taiwan International Graduate Program, Institute of Biomedical Sciences, and [§]Chemical Biology and Molecular Biophysics Program, Taiwan International Graduate Program, Institute of Chemistry, Academia Sinica, No.128, Sec. 2, Academia Road, Nankang, Taipei 11529, Taiwan. [¶]Graduate Institute of Life Sciences, National Defense Medical Center, No. 161, Sec. 6, Minquan E. Road, Neihu, Taipei 11490, Taiwan. [□]Department of Chemistry, National Taiwan University, No. 1, Sec. 4, Roosevelt Road, Taipei 10617, Taiwan.

[*]**Correspondence to**: Joseph Jen-Tse Huang; Institute of Chemistry, Academia Sinica: No.128, Sec. 2, Academia Road, Nankang, Taipei 11529, Taiwan.
Tel: 886-2-27898652
Fax: 886-2-27831237
E-Mail: jthuang@chem.sinica.edu.tw

Supplementary Methods

Plasmid constructions

The GFP constructs from pIVEX2.3d-GFP (Promega) were mutated (Thr^2 to Ala^2 and Lys^3 to Arg^3) by QuickChange™ PCR-mediated site-directed mutagenesis kit (Stratagene Inc.) and served as our protein template. Three polyalanine (poly-A) constructs (2A, 8A, and 17A), each containing a nine alanine substitution, and two constructs, containing the N-terminal signal sequences from LepB (SA) and β-lac (SS) (1), were engineered on to the GFP construct by applying overlap extension PCR (2). The amplicons were further ligated between *Nco*I-*Xma*I restriction enzyme sites in pIVEX2.3d-GFP2A3R vector. In addition, three other constructs ($2A^+$, $8A^+$, and $17A^+$) that included six additional amino acids of the parent sequences right behind the 9 alanine inserts in 2A, 8A, and 17A were obtained by applying site-directed mutagenesis on the poly-A containing plasmids. All the constructs were sequenced by Tri-I Biotech, Inc (Taiwan). The GFP-derivative sequences examined in this study are as follows with the modifications underlined.

GFP_{1-34} (sG):
MARGEELFTGVVPILVELDGDVNGHKFSVSGEGE
GFP_{1-34}-$2Ala_9$ (2A):
MAAAAAAAAAVVPILVELDGDVNGHKFSVSGEGE
GFP_{1-34}-$8Ala_9$ (8A):
MARGEELAAAAAAAAAELDGDVNGHKFSVSGEGE
GFP_{1-34}-$17Ala_9$(17A):
MARGEELFTGVVPILVAAAAAAAAAKFSVSGEGE
GFP_{1-40}-$2Ala_9$ ($2A^+$):
MAAAAAAAAAEELFTGVVPILVELDGDVNGHKFSVSGEGE
GFP_{1-40}-$8Ala_9$($8A^+$): MARGEELAAAAAAAAAVVPILVELDGDVNGHKFSVSGEGE
GFP_{1-40}-$17A_9$($17A^+$): MARGEELFTGVVPILVAAAAAAAAAGDVNGHKFSVSGEGE
SA-GFP (SA):
MANMFALILVIATLVTGILWCVNGHKFSVSGEGE
SS-GFP (SS):
MFRTTLCALLITASCSTFAGDVNGHKFSVSGEGE

The designed primers for establishing these mutants are listed in Table S1.

Overproduction and purification of recombinant trigger factor

Expression of the recombinant protein was carried out following the reported protocol (3). pET21a(+)-TF construct possessing a C-terminal His-tag was

transformed into *E. coli* BL21 (DE3) and over-expression was induced by isopropyl-β-Dthiogalactopyranoside (IPTG, 1 mM). Cells were lysed by French Press in binding buffer (20 mM phosphate buffer, 0.5 M NaCl, pH 7.4) and the targeted protein was isolated and collected by Ni^{2+}-affinity column (GE Healthcare) chromatography with elution buffer (binding buffer with an addition of 50 mM imidazole).

After desalting and concentration with Amicon Ultra (Millipore), the TF-His tagged protein was purified by Superdex75 column (10/300 GL, GE Healthcare). The purified protein was characterized by mass analysis (ESI-MS) and western blotting with a rabbit *anti*-TF-tag pAb (Genscript), and was quantified by the Bradford method (Sigma-Aldrich) using bovine serum albumin (BSA) as a standard.

Sequence analysis of the nascent polypeptides

The total hydrophobicity of the nascent polypeptide sequences was obtained by using MPEx program on the Wimley-White scale (4). The local hydrophobicity curves were generated by calculating the averaging values over a window of 11 residues in the sequences on the Roseman's hydropathy scale (5). The helix propensity was represented as $\Delta(\Delta G)$ relative to Ala, which was assigned the value of zero given its most favorable helix propensity (6).

Supplementary Tables

Table S1 DNA sequences of primers and *anti*-oligonucleotides

Name	Sequence
K3R-f	5' ggAgATATACCATgACTAgAggTgAAgAACTTTTCAC 3'
K3R-r	5' gTgAAAAgTTCTTCACCTCTAgTCATggTATATCTCC 3'
T2A-f	5' AgAAggAgATATACCATggCTAgAggTgAAgAACTTT3'
T2A-r	5' AAAgTTCTTCACCTCTAgCCATggTATATCTCCTTCT 3'
PolyA-N-f	5' gAgACggTCACAgCTTgTCTg 3'
PolyA-C-r	5' TTATgCTAgTTATTgCTCAgCggTg 3'
$2A_9$-f	5'CATgCCATggCTgCAgCTgCTgCAgCCgCAgCggCTgTTgTCCCAATTCTTgTTgAATTAgA 3'
$2A_9$-r	5' TATgCTAgTTATTgCTCAgCggT 3'
$8A_9$-N-r	5' TgCAgCCgCAgCAgCTgCCgCAgCTgCAAgTTCTTCACCTCTAgCCATgg 3'
$8A_9$-C-f	5' TgCggCAgCTgCTgCggCTgCAgAATTAgATggTgATgTTAATgggC 3'
$17A_9$-N-r	5' TgCAgCCgCAgCAgCTgCCgCAgCTgCAACAAgAATTgggACAACTCCAgTg 3'
$17A_9$-C-f	5' gCAgCTgCggCAgCTgCTgCggCTgCAAAATTTTCTgTCAgTggAgAgggTg 3'
SA-f	5' CATggCgAATATgTTTgCCCTgATTCTggTgATTgCCACACTggTgACggg 3' &
	5' CATTTTATggTgCgTgAATgggCACAAATTTTCTgCA 3'
SA-r	5' CAgTgTggCAATCACCAgAATCAgggCAAACATATTCgC 3' &
	5'gAAAATTTgTgCCCATTCACgCACCATAAAATgCCCgTCAC 3'
SS-f	5' CATgTTCCgTACgACgCTCTgCgCCTTATTAATTACCgCCTCTTgCTC3' &

	5' CACATTTgCTggTgATgTTAATgggCACAAATTTTCTgCA 3'
SS-r	5' CggTAATTAATAAggCgCAgAgCgTCgTACggAA 3' &
	5' gAAAATTTgTgCCCATTAACATCACCAgCAAATgTggAgCAAgAgg 3'
$2A^{+}$-f	5’gCTgCAgCCgCAgCggCTgAAgAACTgTTTACCggCgTTgTCCCAATTCTTgTTg 3’
$2A^{+}$-r	5’CAACAAgAATTgggACAACgCCggTAAACAgTTCTTCAgCCgCTgCggCTgCAgC 3’
$8A^{+}$-f	5’CAgCTgCTgCggCTgCAgTggTgCCgATTCTggTggAATTAgATggTgATg 3’
$8A^{+}$-r	5’CATCACCATCTAATTCCACCAgAATCggCACCACTgCAgCCgCAgCAgCTg 3’
$17A^{+}$-f	5’gCAgCTgCTgCggCTgCAggCgATgTgAATggCCATAAATTTTCTgTCAgTgg 3’
$17A^{+}$-r	5’CCACTgACAgAAAATTTATggCCATTCACATCgCCTgCAgCCgCAgCAgCTgC 3’
T86 for SA/SS	5' CACAAATTTTCTgTCAgTggAgAgggTg 3' &
	5' CACCCTCTCCACTgACAgAAAATTTgTg 3'
anti-$sGFP_{34}$	5’-TTCACCCTCTCCACTgACAgA -3’
anti-ssrA	5' TTAAgCTgCTAAAgCgTAgTTTTCgTCgTTTgCgACTA 3'

Table S2 Lifetime measurements of the $BODIPY_{FL}$

Sample	τ_1 (ns)	τ_2 (ns)	f1	f2	$\chi 2$
Blank experiment* with $BODIPY_{FL}$-Lys-$tRNA^{Lys}$	0.6±0.1	5.7±0.1	0.03	0.97	<1.1
Blank experiment with $BODIPY_{FL}$ -Lys-$tRNA^{Lys}$ and $BODIPY_{576}$-Met-$tRNA_f^{Met}$	1	5.8±0.1	0.02	0.98	<1.2
1mM mixture† in MeOH	N.D.				
100 mM mixture in MeOH	3.2	8.2	0.15	0.85	2.5
10 mM mixture in MeOH	-	6.2	-	1	3.3
1 mM mixture in MeOH	-	5.7	-	1	1.3
10 nM mixture MeOH	<0.01	5.7	<0.01	>0.99	0.5
1 nM mixture in MeOH	<0.01	5.6	0.03	0.97	0.6
2nM $BODIPY_{FL}$ in MeOH	<0.01	5.6	0.04	0.96	0.6

* Cell-free reaction without any plasmid

† The mixture includes free BODIPY FL-SE and BODIPY 576/589-SE

Table S3 The f_3/f_2 values predicted with different probe incorporation efficiencies and different extents of unstructured motif in the A_9 fragments in the dual-labeled RNCs

Probe incorporation efficiency (%)*	25					50					75					100				
Extent of the extended conformation (%)	0	25	50	75	100	0	25	50	75	100	0	25	50	75	100	0	25	50	75	100
f_3/f_2	0.2	0.15	0.09	0.04	0	0.37	0.25	0.16	0.08	0	0.5	0.33	0.2	0.09	0	0.62	0.4	0.23	0.11	0
*Analysis assumes that the efficiencies of incorporating both the donor and acceptor probes into the nascent chains are the same.																				

TABLE S4 Lifetime measurements of the fluorescent RNCs

Fluorophore-nascent chain in RNC	Lifetime (ns)*			Fraction of Intensity				
	τ_1	τ_2 (τ_F^D)	τ_3 (τ_F^{D+A})	f_1	f_2	f_3	χ^2	E_{FRET}†
D-sG	<1.2	5.8±0.1	-	0.03	0.97	-	<1.3	-
DA-sG		5.9±0.1	-	0.03	0.97	-	<1.9	-
D-2A		5.8±0.1	-	0.04	0.96	-	<1.6	-
DA-2A		5.8±0.1	4.4±0.3	0.05	0.73	0.23	<1.7	0.3±0.1
D-2A$^+$		5.9±0.1	-	0.10	0.90	-	<1.7	-
DA-2A$^+$		6.0±0.1	-	0.10	0.90	-	<1.7	-
D-8A		5.9±0.1	-	0.03	0.97	-	<1.6	-
DA-8A		5.9±0.1	4.2±0.1	0.03	0.85	0.12	<1.1	0.3±0.1
D-8A$^+$		6.1±0.1	-	0.08	0.92	-	<1.6	-
DA-8A$^+$		6.1±0.1	-	0.07	0.93	-	<1.7	-
D-17A		5.9±0.1	-	0.02	0.98	-	<1.6	-
DA-17A		6.0±0.1	4.1±0.7	0.02	0.67	0.31	<1.2	0.3±0.1
D-17A$^+$		6.1±0.1	-	0.07	0.93	-	<1.7	-
DA-17A$^+$		6.1±0.1	-	0.08	0.92	-	<1.7	-

*The lifetimes shown are means ± SD. The total number of measurements from independent experiments, n, is 3-6. †The energy transfer efficiency, E_{FRET}, was calculated from Eq. 9: $E_{FRET} = 1/[1+(R/R^0)]^6$. According to the *P* value in *t*-test, the τ_F^{D+A}s measured from the poly-A samples were significantly different from their corresponding τ_F^Ds ($P \leq 0.001$).

Table S5 Ratio of the TF recruitment*

Nascent chain in RNC	Supplement of TF (μM)			
	1	2	3	4
sG	0.81±0.04	0.87±0.09	0.87±0.10	1
2A	0.32±0.02	0.46±0.21	0.58±0.15	0.86±0.19
8A	0.17±0.04	0.45±0.09	0.46±0.15	0.69±0.12
17A	0.56±0.08	0.85±0.09	0.94±0.08	0.93±0.29
SA	-	0.17±0.06	-	0.31±0.06
SS	-	0.30±0.11	-	0.59±0.16
$2A^+$	-	0.69±0.08	-	0.78±0.12
$8A^+$	-	0.42±0.13	-	0.76±0.15
$17A^+$	-	0.67±0.09	-	0.85±0.06

*Ratios were obtained by comparing the recruited TF to the system examined against the recruitment by sG under the conditions of the highest recruitment, which was obtained with the sG at 4 μM supplemented TF.

Supplementary Figures

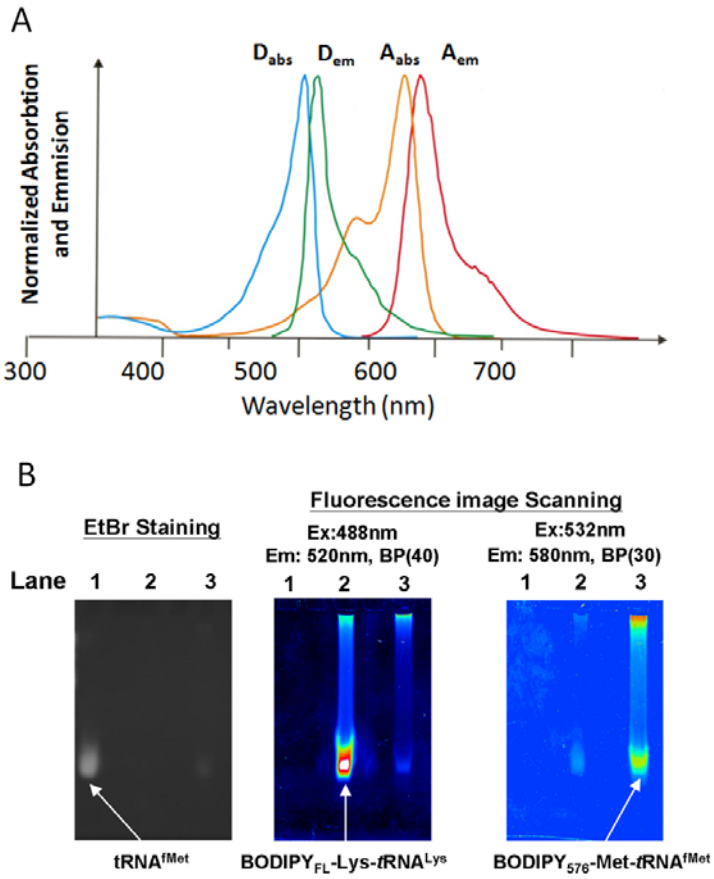

Figure S1 Fluorescent properties of the fluorophores and the fluorophore-attached tRNAs. (A) The absorption (abs) and emission spectra (em) of the BODIPY FL-SE (D) and BODIPY 576/589-SE (A). (B) The PAGE analysis of the Met-$tRNA_f^{Met}$ (Lane 1), donor-labeled tRNA (Lane 2), and acceptor-labeled tRNA (Lane 3) visualized by EtBr staining or fluorescence scanning on 10% NaOAc-urea-PAGE.

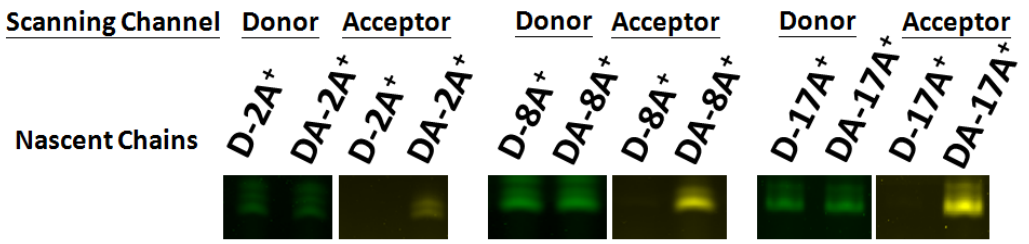

Figure S2 Fluorescent scanning of the fluorophore-labeled RNCs on Tris-acetate SDS-PAGE. The scanning was performed on single- (D) or double- (DA) labeled poly-A^+ nascent chains. The donor was excited at 470 nm and detected at 520 nm; and the acceptor was excited at 532 nm and detected at 580 nm.

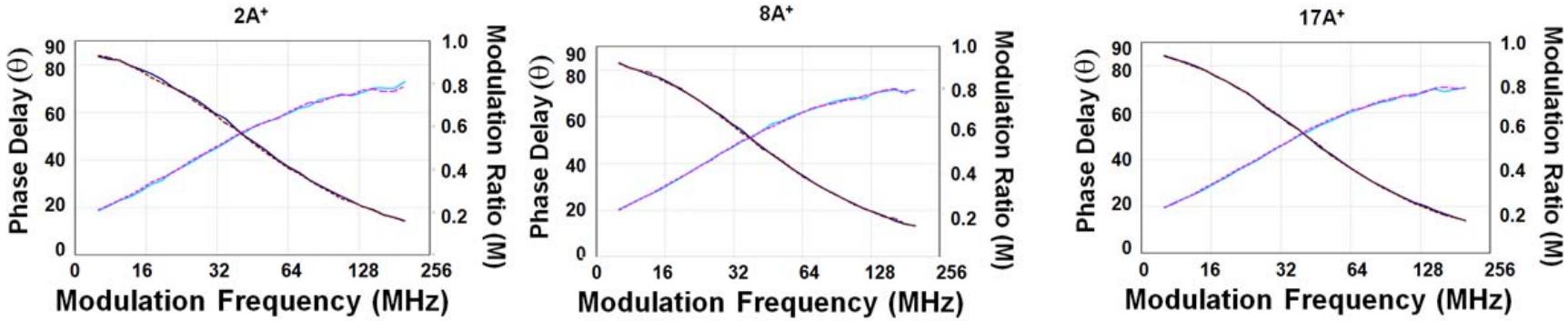

Figure S3 Lifetime measurements of the polyA$^+$-RNCs (2A$^+$, 8A$^+$, and 17A$^+$) determined by frequency-domain fluorimeter. Data are shown for the donor-labeled samples (solid line) and donor-acceptor double-labeled samples (Dash line). Details of the fluorophores and their lifetimes that fitted the experimental measurements for the various nascent chains are reported in Table S3.

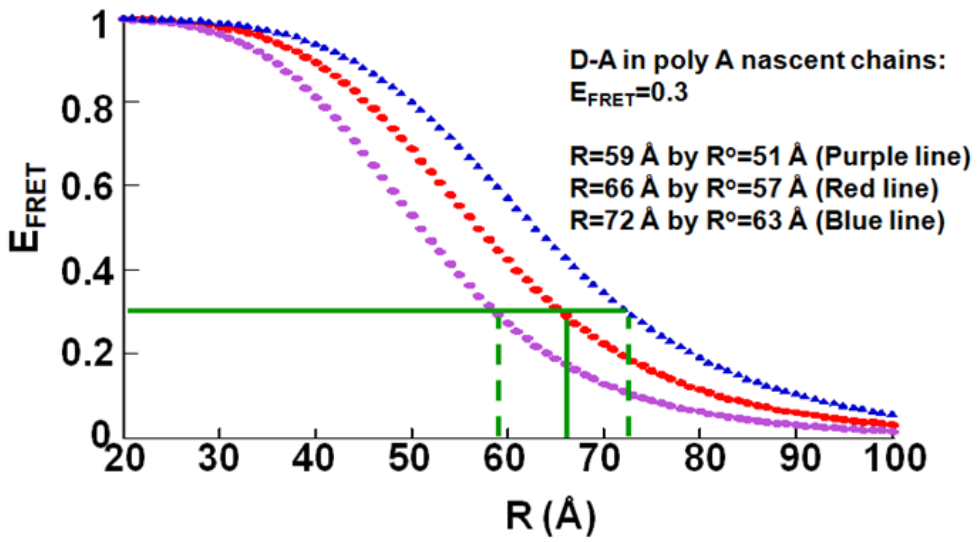

Figure S4 The dependence of the energy transfer efficiency on donor-acceptor distance. The predictions are based on three values of R^0s for the donor-acceptor pair including the value R^0=57 Å (red line) used in the study as well as the values of R^0s corresponding to ±10% uncertainty (R^0=51 Å, purple line; R^0= 63 Å, blue line). The relationship between the observed E_{FRET} and the corresponding distance separating the FRET donor-acceptor pair is given by $E_{FRET} = 1/[1+(R/R^0)]^6$. It has been reported earlier that the anisotropy of 0.25 for the donor and 0.3 for the acceptor may yield a maximum range of 0.1-3.1 for κ^2, yielding a –25% to +29% maximum uncertainty in R^0 due to the orientation effects (7). However, the actual uncertainty is closer to ±10%, largely because of the statistical improbability of some dye orientations and the flexibility of the dye tethers (7). From our determination, the fluorescent anisotropy of the labeled donor on the nascent chains within tunnel is about 0.18, which suggests that the probe has a significant freedom of rotation. The possible dynamics of the probes associated with the nascent polypeptide may cause about 13 Å uncertainty in the determination of the donor-acceptor distance R for a sample with E_{FRET} of 0.3 if the uncertainty in R^0 is ±10%. Note that this uncertainty in R does not in any way affect the overall conclusions of the study, since E_{FRET} is the same (0.3±0.1) for the nascent chains in the fluorescent RNCs 2A, 8A and 17A.

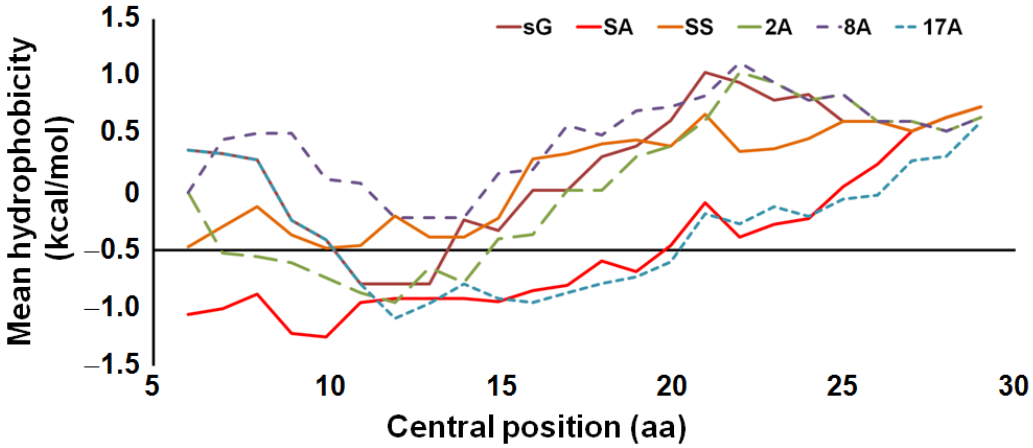

Figure S5 The mean hydrophobicity curve of sG, 2A, 8A, 17A, SA, and SS. The mean hydrophobicity was obtained by averaging the hydrophobic scores of 11 residues in each of the polypeptides on the Roseman's hydropathy scale (5) and reported at the central amino acid within the scanned residues. Values lower than –0.5 kcal/mol represent high hydrophobicity (8).

Supporting References

1. Bornemann, T., J. Jockel, M. V. Rodnina, and W. Wintermeyer. 2008. Signal sequence-independent membrane targeting of ribosomes containing short nascent peptides within the exit tunnel. Nat. Struct. Mol. Biol. 15:494-499.
2. Lee, J., M. K. Shin, D. K. Ryu, S. Kim, and W. S. Ryu. 2010. Insertion and deletion mutagenesis by overlap extension PCR. Methods Mol. Biol. 634:137-146.
3. Lin, K. F., T. R. Lee, P. H. Tsai, M. P. Hsu, C. S. Chen, and P. C. Lyu. 2007. Structure-based protein engineering for alpha-amylase inhibitory activity of plant defensin. Proteins 68:530-540.
4. Wimley, W. C., and S. H. White. 1996. Experimentally determined hydrophobicity scale for proteins at membrane interfaces. Nat. Struct. Biol. 3:842-848.
5. Roseman, M. A. 1988. Hydrophilicity of polar amino acid side-chains is markedly reduced by flanking peptide bonds. J. Mol. Biol. 200:513-522.
6. Pace, C. N., and J. M. Scholtz. 1998. A helix propensity scale based on experimental studies of peptides and proteins. Biophys. J. 75:422-427.
7. Woolhead, C. A., P. J. McCormick, and A. E. Johnson. 2004. Nascent membrane and secretory proteins differ in FRET-detected folding far inside the ribosome and in their exposure to ribosomal proteins. Cell 116:725-736.
8. Kaiser, C. M., H. C. Chang, V. R. Agashe, S. K. Lakshmipathy, S. A. Etchells, M. Hayer-Hartl, F. U. Hartl, and J. M. Barral. 2006. Real-time observation of trigger factor function on translating ribosomes. Nature 444:455-460.